Comparison of System-Level Availability in Industrial Grids

G. Emmers, J. Driesen
KU LEUVEN, Department of Electrical Engineering, ELECTA - ENERGYVILLE
Kasteelpark Arenberg 10
3001 Leuven, Belgium
Phone: +32 (0) 16-379165
Email: glenn.emmers@kuleuven.be

Acknowledgments

This work is performed as part of the MultiDC-ICON project, HBC.2019.0084. Funded by the Institute for the Promotion of Innovation through Science and Technology in Flanders (VLAIO) and Flanders Make, the strategic research center for the manufacturing industry in Belgium.

Keywords

≪LVDC≫, ≪Reliability≫, ≪Industrial Application≫, ≪Uninterruptible Power Supply (UPS)≫

Abstract

This paper evaluates the availability of traditional AC based and state-of-the-art LVDC based industrial grids. The main focus is on industrial grids with a high penetration of power electronics, used to power production lines with many drives. Firstly, the Monte Carlo approach is presented to analyze the availability of several grid topologies relevant to industry. Secondly, this method is used to validate a Multi-State Markov approach. The Multi-State Markov approach is extended with a battery dependency model, to incorporate battery life in the analysis. Finally, after validation, the Multi-State Markov approach is used to determine the influence of the AC grid availability and the battery backup time on the availability of the presented use cases. LVDC systems prove to be more available at the load connection points and, depending on converters chosen, also have the potential to outperform UPS systems at distribution board level.

Introduction

In recent years, the interest in DC has been growing because, compared to a traditional AC exploitation, there is a potentially increased efficiency, an increased transmission capacity and an increase in compatibility with modern loads and storage [1]. Especially in industry, the dependency on variable speed drives has grown significantly, with the main drivers being the increased efficiency and the decreased CAPEX due to less conversion steps [2]. These variable speed drives introduce a DC step in between the two AC systems. Oftentimes multiple back-end DC/AC converters are connected to a single front-end AC/DC converter creating a larger DC bus to facilitate regenerative braking. When building further upon this concept, the logical next step is the implementation of a battery on the DC bus. Adding a battery to an industrial grid offers plenty of advantages, such as distributed UPS properties for the entire grid to increase the system availability and peak shaving when the power system demand is characterized by short but high power peaks [3]. These peaks are crucial for the design, exploitation and cost of the electrical network [4]. Not only is the electrical network designed to supply the peak power, in some cases industrial customers are also charged by their maximum power demand. The adaptation of LVDC technology allows for a simple and efficient implementation of battery storage on the DC bus. This storage can then be used to flatten the load curve, where energy is stored during periods of low demand and released during periods of higher demand [5].

Besides the peak shaving aspect, a battery significantly increases the availability of an LVDC network, making it act as a UPS system. The battery will isolate the DC grid from anything happening on the AC side, creating fault ride-through capabilities. Many industrial systems are plagued with very short-term interruptions (<1s), which are statistically not recorded but occur significantly more frequently than unplanned supply interruptions of more than three minutes [6]. Additionally, these LVDC power systems can be significantly larger in size and power than a UPS system, covering more loads [7].

New in this paper is the comparison of a traditional AC based industrial grids with new and unconventional LVDC based industrial grids, with a special focus on the effects of battery backup time and AC grid availability in the availability analysis of all systems considered. Conclusions can be drawn based on how the amount of power electronic conversion steps influence the system availability and how redundancy can be used to increase the system availability, yet using less components than traditional solutions.

This paper first describes the mathematical framework used to evaluate the systems under consideration. Next follows a description of the four system architectures under consideration and the analyses performed. Finally, the paper is ended with a conclusion.

Mathematical framework

This section starts with discussing the assumptions made regarding the reliability modeling, followed by providing the two methodologies used to analyze the availability of the selected use cases, to finish with a definition of system failure.

Reliability modeling

The analysis presented in this paper includes several assumptions to keep the model concise and tractable. These assumptions are the following:

- All components are independent from each other and can be modeled as a two state Markov process.
- Given that the components can be modeled as a two state Markov process, it is assumed that each component i has a constant failure rate λ_i (failures/hr) and a constant repair rate μ_i (repairs/hr), which means they have an exponential distribution. This is true under the assumption that all equipment is operational in their useful life, rather than the wear-out phase or the phase of infant mortality.
- Batteries with finite charge cannot be modeled as a two state Markov process, therefore another assumption regarding the incorporation of battery life in the availability modeling is required.
- System unavailability U_s can be calculated as the probability where down-time in the battery power supply exceeds battery reserve time. The battery power supply consists of the main power supply, distribution transformer, a front-end rectifier and in some cases a DC/DC converter. In [10] this is presented as follows:

$$U_s = \lambda_A \int_T^\infty f_A(t)dt \frac{\int_T^\infty (t-T) f_A(t)dt}{\int_T^\infty f_A(t)dt}$$

  With λ_A the failure rate of the battery power supply, $f_A(t)$ the probability density function of the failure duration time and T the battery reserve time. If the probability density function is then dissolved in terms of each element that is part of the battery power supply, this leads to:

$$U_s = \sum_{k=1}^{n} U_k e^{-\mu_k T}$$

  With n the amount of components part of the battery power supply and U_k the unavailability of this component. In this paper T is initially considered to be five hours, after validation of the model T is varied to analyze its influence.
- One and only one transition can occur at a given time instant t.

- After the repair of one out of two components that were in a faulty state together, the other component is assumed to be repaired before the firstly repaired component fails again. This assumption is made to allow the battery to at least partially recharge once it has run out of charge.
- Availability as used in this paper is considered to be the steady state availability, which is defined to be the limit of the instantaneous availability for time going to infinity [11]. This availability can be expressed as $A = \frac{MTBF}{MTBF+MTTR}$, with MTBF the Mean Time Between Failures ($\frac{1}{\lambda}$) and MTTR the Mean Time To Repair ($\frac{1}{\mu}$). Consequently, the availability can also be expressed in terms of the failure rate and the repair rate as: $A = \frac{\mu_i}{\mu_i+\lambda_i}$. Typically, steady state availability is specified in nines notation, where the number of nines represents the amount of nines in the fraction of time that the system is available [12]. Table I gives an overview of the availability specified in nines notation and its corresponding downtime.

Table I: Availability and downtimes [13]

Availability (number of 9s)	Downtime per year	Downtime per day
1	36.5 days	2.4 hours
2	3.65 days	14.4 minutes
3	8.76 hours	1.44 minutes
4	52.56 minutes	8.66 seconds
5	5.26 minutes	864.3 milliseconds

Methodologies

Many options exist when it comes to performing a reliability analysis of electrical installations with Markovian properties. The most common ones are the reliability block diagram or the fault tree analysis, especially when the systems under consideration are relatively small and calculations are simple to perform. As systems get larger, these analytical methods become tedious to solve. For that reason the Universal Generating Operator (UGO) approach is used, which is a method for solving a Multi-State problem. The assumptions made above limit us to the use of Markov-models, including a battery in this analysis would ideally require a semi-Markov approach, which is a significantly more difficult problem to set up. Alternatively the method described above is used to estimate the system unavailability due to an empty battery. Because the results based on this battery unavailability model as described above are an estimate, the results found with the UGO are validated with a Monte Carlo Simulation (MCS). In contrary to the UGO, the MCS is a time-based solution to the availability analysis rather than a stochastic one. This heavily simplifies the implementation of time-dependent problems, such as the battery problem at hand. The disadvantage of the MCS approach, compared to the UGO approach, is the time it takes to solve the problem. Solving a UGO can be done within a time span of seconds to minutes, whereas an MCS approach can take up to several minutes to hours, depending on the size of the system to solve and the accuracy required.

Universal Generator Operator

The UGO technique is used to calculate a Multi State System performance distribution based on the stochastic performance of the elements forming that system. What makes the UGO technique so unique is the fact that this approach uses simple recursive procedures and makes complicated combinatorial algorithms obsolete by providing a systematic method for enumerating the systems states [14].

The performance of any element e in the system is represented by a Universal Generating Function:

$$\omega_e(z) = \sum_{s \in S} p_s \cdot z^{v_s}$$

With S the state-space including its unique performances v_s and p_s the associated probabilities[15]. In the case of this analysis, the unique performances of the elements are taken to be the minimum and the maximum power level. These power levels then have their respective probability associated to them. The

probabilities for each state are calculated for each component separately in its designated Markov model. In this analysis every component has two states, each determined by a constant failure rate and a constant repair rate, which in turn determines the final states probabilities.
To find the system performance at a specific point in the network, the Universal Generating Operator Ω can be constructed, based on the methodologies presented in [14]:

$$\Omega_u([\omega_e(z)]) = \sum_{s_1}^{S_{e_1}} \cdots \sum_{s_n}^{S_{en}} (p_{s_1} \cdot \ldots \cdot p_{s_n}) \cdot z^{f^{str}(v_{s_1,\ldots,s_n})}$$

With f^{str} the structure function to express the performance towards that specific point in the system[15]. To implement the battery backup time into the UGO, the method as discussed in Section "Reliability modeling" is used. This leads to an additional unavailability of the system, which is equal to an additional probability for the system to be in either an unavailable or an available state in the steady state solution. The new probabilities following from the calculated unavailability, are treated as the solved state transition diagram of an extra component, which can be placed at the position of the distribution board in the grids described in the next section. All UGO analyses are performed using MULTISTATESYSTEMS.JL[1], a JULIA package developed to solve multi-state systems.

Monte Carlo Simulation

The validation of the results generated with the UGO are performed with a Monte Carlo Simulation in MATLAB as presented in [16]. The chosen implementation is the Direct Simulation Method, which samples the transition times of all elements individually. The element with the shortest transition time is then selected to be the one to make the transition at that moment t. This particular implementation of the MCS allows for simple time-dependent adjustments, such as the time dependency of the battery state. The algorithm was extended to change the battery state from as soon as the state transition time went beyond the battery backup time, in this case five hours. To perform the MCS several minimal cut sets have to be defined, which will be elaborated upon in the next section.

Case study

Systems in comparison

In this section four different topologies are presented, the first two of which are traditional AC implementations, followed by two state-of-the-art LVDC implementations.

Conventional AC distribution system

The first system under consideration is the conventional AC distribution system as shown in Fig. 1. This system is connected to the main power supply through a distribution transformer, followed by a distribution board towards the different machines, which contain variable speed drives (VSD's). Typically these VSD's contain a two-stage power electronic conversion, with a front-end AC/DC converter connected to the AC distribution to create an internal DC bus, which in turn feeds a back-end DC/AC inverter to supply the motors of the machines. In case machines contain multiple drives, it is common practice to connect these back-end converters to a common active front-end. This benefits overall system efficiency as recovered braking energy is directly used by another drive.

Conventional AC UPS distribution system

The second system under consideration is the conventional AC distribution system with an additional UPS as shown in Fig. 2. In this case the system consists of the traditional AC distribution, but critical machines are being connected through a UPS installation. This increases the resilience against grid-side disturbances, but is detrimental to the system efficiency. Many types of UPS-setups exist, but the most common one is a static double-conversion type. This type of UPS consists of an AC/DC converter feeding a DC bus, to which a battery and a DC/AC inverter are connected [8].

[1] Available at https://github.com/timmyfaraday/MultiStateSystems.jl

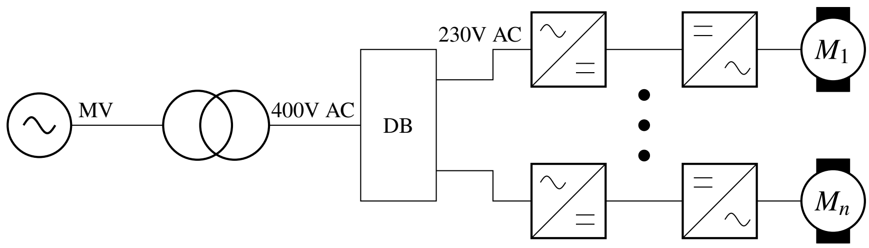

Fig. 1: Conventional AC distribution system.

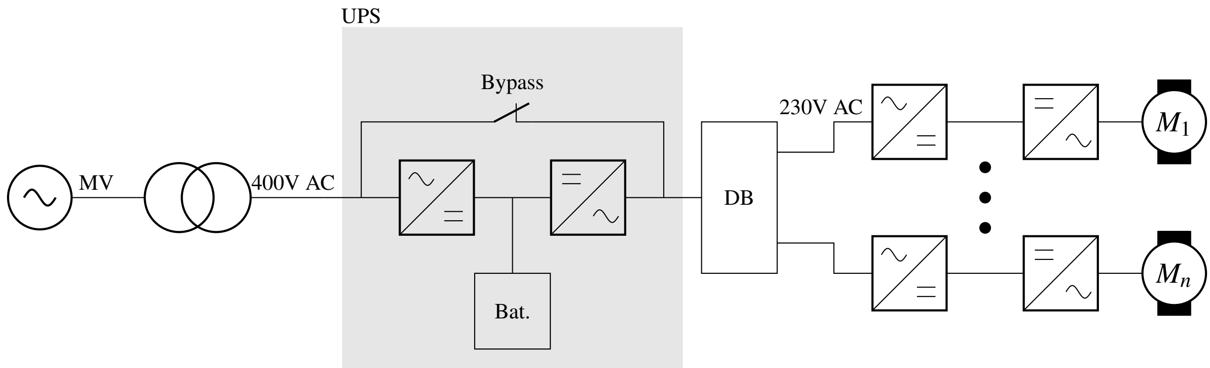

Fig. 2: Conventional AC distribution system with UPS.

LVDC distribution system

The third system under consideration is the LVDC distribution system as shown in Fig. 3. This system architecture extends the benefits of a common DC bus as seen for the conventional AC distribution system, towards the entire plant. Not only is energy transfer possible within a machine, energy transfer between machines is facilitated as well. Fewer conversion steps are required and common components such as filters and capacitors are eliminated. Furthermore, there is an ever decreasing cost of electrical storage, which allows to incorporate storage either centrally or per machine [7],[9]. This allows to add UPS properties to the entire system, comparable to the AC UPS case, but with a significantly lower amount of converters required. Notice that the converters in a DC system can be smaller in power level than for AC systems, because power transfer between several components is facilitated and the battery can be used for peak shaving.

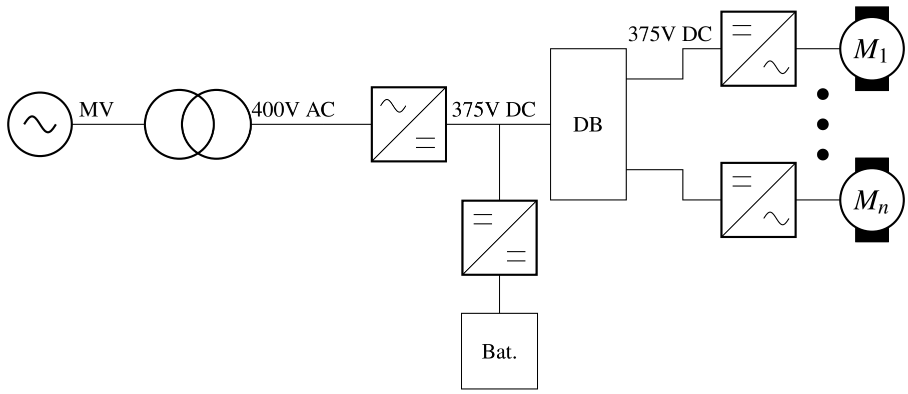

Fig. 3: State-of-the-art LVDC distribution system.

Redundant LVDC distribution system

Finally, the previously described LVDC distribution system is extended with a redundant front-end AC/DC converter, which is shown in Fig. 4. LVDC systems are highly modular, which makes it easy to add an additional AC/DC converter for extra redundancy. By doing so, the front-end as single point of failure is eliminated and the degrees of redundancy of the AC UPS case and the LVDC case are leveled out, which makes for a fair comparison. Whereas the AC UPS case has a path through the bypass switch, the front end and the battery, the redundant LVDC case has a path through two front-ends and the battery. By adding an extra converter to the system, the influence of redundancy before the distribution board is investigated.

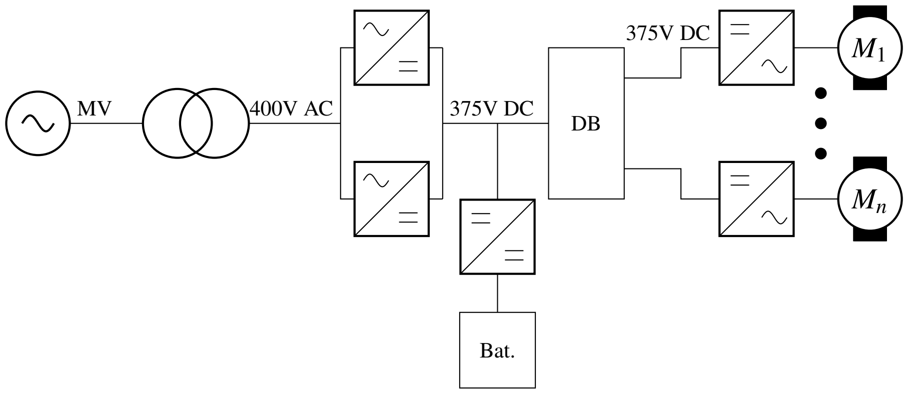

Fig. 4: State-of-the-art redundant LVDC distribution system.

Availability Analysis

System Failure Definition

Two points of interest are investigated in the further analysis of the systems under investigation. The first point of interest is the availability of the distribution system at the distribution board, indicated by DB in the figures above. It is important to take into account that the characteristics of the power available at the distribution board are different for AC systems and DC systems. As a consequence, it is impossible to connect DC loads directly to an AC distribution board and vice versa. The second point under investigation is the load itself, which is the main concern of the system exploiter. The system is said to be available as long as it is in a state to perform as required, meaning the distribution board or the load gets power of a sufficient quality. Table II shows the failure rates and repair rates of the components under consideration in this analysis, expressed in failures per hour and repairs per hour respectively.

Table II: Reliability Data [8]

Component	i	λ_i (f/hr)	μ_i (r/hr)
Main Power Supply	MPS	0.0003142	0.8058
Bypass Switch	SW	4.2166700e-6	0.4269
Battery	BAT	2.0722222e-6	0.0658
Distribution Transformer	DT	8.5777778e-6	0.9552
Front-end Rectifier	FE	2.9666667e-6	0.1400
Inverter/Rectifier	INV	2.3305555e-6	0.0936
DC/DC Converter	DC	8.0580000e-6	0.1250

Universal Generating Operator

The availability analysis with the UGO requires the additional unavailability caused by an empty battery to be calculated manually. An illustrative example applied to the AC UPS case follows below. The battery is the single power source in case one of the following events occur:

- Grid failure
- Transformer failure
- Bypass switch failure & front-end failure

This leads to the following calculations, as presented in section "Reliability Modeling":

$$U_1 = U_{MPS} e^{-\mu_{MPS} * 5}$$

$$U_2 = U_{DT} e^{-\mu_{DT} * 5}$$
$$U_3 = U_{FE} U_{SW} e^{-\mu_{SW} * 5}$$
$$U_s = \sum_{k=1}^{3} U_k$$

A first thing to note is the choice to only incorporate the repair-rate of the bypass switch in the equation for the unavailability (U_3) caused by the simultaneous bypass switch and front-end failure. The reasoning behind this is that the bypass switch has the highest repair-rate and that the system will be operational once this component is repaired. Secondly, it is also assumed that the front-end is repaired before the switch fails again. Next, the DC/DC converter is not included in these calculations for cases that have a DC/DC converter as part of the battery power supply. This is justified because the state of charge of the battery will not change in case the DC/DC converter fails, consequently the battery cannot act as backup power supply. Finally, the calculated unavailability is then added in series of the distribution board unavailability within the UGO. As mentioned before, the UGO analysis is performed with JULIA package MULTISTATESYSTEMS.JL[2].

Monte Carlo Simulation

The implementation of the MCS as described above, requires minimal cut sets to be defined for the cases under investigation. Table III gives an overview of the minimal cut sets defined for each case, which is a combination of elements that cause the system to become unavailable when being in a failed state. The abbreviations used in Table III can be found in Table II. The failure of the battery includes both failure states; broken battery or out of charge. The table-elements marked in gray indicate the additional cut sets used to investigate the availability at the load.

Table III: Minimal Cut Sets for the MCS implementation

AC cut sets	UPS cut sets	LVDC cut sets	LVDC Red. cut sets
$\{MPS\}$	$\{MPS, BAT\}$	$\{MPS, BAT\}$	$\{MPS, BAT\}$
$\{DT\}$	$\{MPS, INV_{UPS}\}$	$\{MPS, DC\}$	$\{MPS, DC\}$
$\{INV_{ac/dc}\}$	$\{DT, BAT\}$	$\{DT, BAT\}$	$\{DT, BAT\}$
$\{INV_{dc/ac}\}$	$\{DT, INV_{UPS}\}$	$\{DT, DC\}$	$\{DT, DC\}$
	$\{SW, BAT\}$	$\{FE, BAT\}$	$\{FE1, FE2, BAT\}$
	$\{SW, INV_{UPS}\}$	$\{FE, DC\}$	$\{FE1, FE2, DC\}$
	$\{INV_{ac/dc}\}$	$\{INV_{dc/ac}\}$	$\{INV_{dc/ac}\}$
	$\{INV_{dc/ac}\}$		

Results and discussion

Table IV and Table V show the results of the UGO method and MCS method respectively, both with a battery backup time of five hours and an AC mains grid availability of three nines. The results of both methods are not the exact same, but they are definitely close enough to consider them equal. Consequently, the MCS method not only validates the UGO method, it also proves that the implementation of the battery life as such, is an appropriate method to consider battery life without using more complex semi-Markov methods.

The results clearly show that the AC implementation has the lowest availability, both at the distribution board and at the load, although the discrepancy at the load decreases relative to other setups. This is because the AC grid availability is more dominant in this analysis than the converter reliabilities, therefore contributing less to the overall availabilities calculated. Next, the new LVDC implementation has the lowest availability at the distribution board out of the final three topologies, leading to more system-wide outages. This is explained by the level of redundancy, which is lower than for the AC UPS

[2] Available at https://github.com/timmyfaraday/MultiStateSystems.jl

Table IV: Availability Data Resulting From UGO

System (UGO)	At Distribution Board		At Load	
	Availability	Unavailability	Availability	Unavailability
Standard AC	3 nines	39.876e-5	3 nines	44.853e-5
AC UPS	5 nines	0.7032e-5	4 nines	5.6822e-5
LVDC	4 nines	1.7497e-5	4 nines	4.2336e-5
Redundant LVDC	5 nines	0.6972e-5	4 nines	3.1867e-5

Table V: Availability Data Resulting From MCS

System (MCS)	At Distribution Board		At Load	
	Availability	Unavailability	Availability	Unavailability
Standard AC	3 nines	39.889e-5	3 nines	44.905e-5
AC UPS	5 nines	0.7068e-5	4 nines	5.6638e-5
LVDC	4 nines	1.7441e-5	4 nines	4.2474e-5
Redundant LVDC	5 nines	0.6949e-5	4 nines	3.2139e-5

case and the redundant LVDC case. Yet, the unavailability of the load is lower for the LVDC case than for the AC UPS case. The reduction in converters pays off towards the end of the distribution chain. Finally, the redundant LVDC case has the lowest unavailability by a very small margin. Both the AC UPS and the redundant LVDC system have a similar level of redundancy, which translates into similar levels of availability at the distribution board level. The difference is larger at the load level, once more because of the reduced amount of converters in the DC case. Beware that the system integration and exploitation cost for both LVDC system is significantly lower than for the AC UPS case, driven by a lower amount of installed conversion steps.

Battery life dependency

The results so far were calculated using a constant battery life and a constant AC grid availability. In this section, the results show the dependency on battery backup time. Because the MCS method requires significantly more time to solve than the UGO method, this analysis is performed using the validated UGO method exclusively. Fig. 5 shows the availability at (a) distribution board and (b) load level on a logarithmic scale and a linear scale respectively, for a battery backup time ranging from 1 hour to 50 hours. Fig. 5 (a) shows that the battery backup time has an influence on the distribution board availability until a battery backup time of about 15 hours for both the AC UPS case and redundant LVDC case. The battery life has a much larger influence on the availability of the standard LVDC case, which is caused by the front-end as single point of failure. The small difference in availability between the AC UPS case and the redundant LVDC case beyond 15 hours of battery life is explained by a difference in reliability of the DC/AC converter on the one hand and the DC/DC on the other hand. Fig. 5 (b) shows that loads connected to LVDC systems are more available at any battery size, which can be explained by the additional converter between the distribution board and the loads for AC cases.

Variable AC grid availability

This section analyzes the effect of the AC grid availability on the availability of both the distribution board and the load. Fig. 6 (a) shows the unavailabilities of the distribution board for the different cases, including an AC Grid case that reflects the AC grid availability on the DB availability. In essence this mimics a facility where the system operator already made investments to improve the availability of the AC distribution. Interesting about Fig. 6 (a), are the crossover points between the different cases and the AC Grid, indicated where it might or might not be worthwhile to make extra investments on another distribution topology, for a given AC distribution grid availability. The LVDC case has a crossover at around 5 nines, the AC UPS case has a crossover at 7 nines and finally the Redundant LVDC case has a crossover at 13 nines. Each case is more available than the AC grid before the crossover point and less available behind the crossover point. To put this into perspective, even TSO busbar availabilities rarely

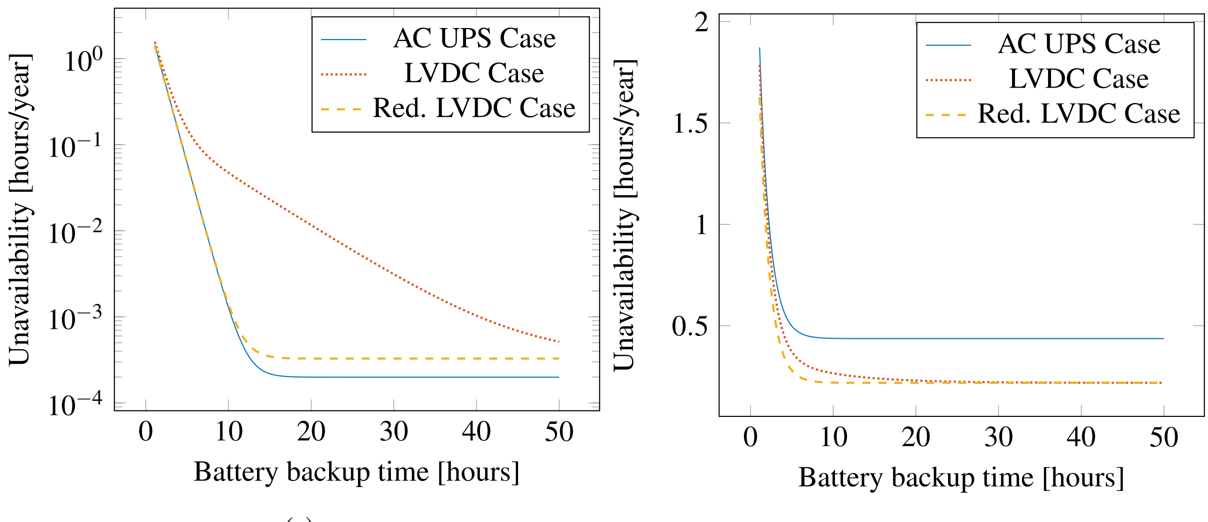

(a) (b)

Fig. 5: Unavailability in hours per year in function of the battery backup time for (a) the distribution board and (b) the loads

go beyond 5 nines. Finally, Fig. 6 (b) shows that for any given AC grid availability, the loads connected to both LVDC cases outperform the loads for the AC cases availability-wise.

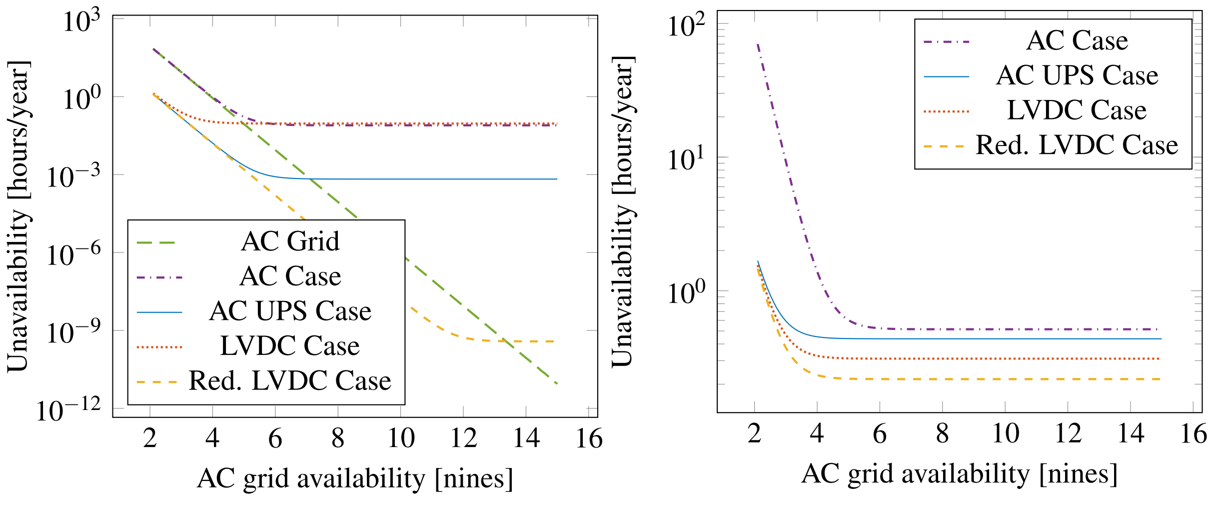

(a) (b)

Fig. 6: Unavailability in hours per year in function of the AC grid availability for (a) the distribution board and (b) the loads

Conclusion

This paper first describes the mathematical framework to perform an availability analysis on industrial distribution grids. In this analysis a method to include battery backup time in a Universal Generating Operator methodology based on Markov methods is validated using a Monte Carlo Simulation. The results of both methods show promising results regarding the availability of loads in LVDC grids, compared to existing AC implementations. Finally, the analysis performed with the UGO method exclusively shows the influence of both the battery backup time and AC grid availability on both the distribution board availability and the load availability. These results show that LVDC implementations, with a significantly smaller component count, have the potential to outperform AC solutions at distribution board level and most definitely outperform them at load level.

References

[1] J. J. Justo, F. Mwasilu, J. Lee, and J. W. Jung, "AC-microgrids versus DC-microgrids with distributed energy resources: A review," Renewable and Sustainable Energy Reviews, vol. 24, pp. 387–405, 2013. [Online]. Available: http://dx.doi.org/10.1016/j.rser.2013.03.067

[2] R. Saidur, S. Mekhilef, M. B. Ali, A. Safari, and H. A. Mohammed, "Applications of variable speed drive (VSD) in electrical motors energy savings," Renew. Sustain. Energy Rev., vol. 16, no. 1, pp. 543–550, 2012.

[3] C. Rahmann, B. Mac-Clure, V. Vittal, and F. Valencia, "Break-even points of battery energy storage systems for peak shaving applications," Energies, vol. 10, no. 7, 2017.

[4] Z. Wang and S. Wang, "Grid power peak shaving and valley filling using vehicle-to-grid systems," IEEE Trans. Power Deliv., vol. 28, no. 3, pp. 1822–1829, 2013.

[5] R. Martins, H. C. Hesse, J. Jungbauer, T. Vorbuchner, and P. Musilek, "Optimal component sizing for peak shaving in battery energy storage system for industrial applications," Energies, vol. 11, no. 8, 2018.

[6] Industrie- und Handelskammer in Bayern, "BIHK-Studie: Energiewende im Strommarkt – Versorgungsqualität" 2017.

[7] B. K. Johnson, "An Industrial Power Distribution System Featuring Ups Properties," Ieee, 1993.

[8] V. Sithimolada and P. W. Sauer, "Facility-level DC vs. typical AC distribution for data centers: A comparative reliability study," IEEE Reg. 10 Annu. Int. Conf. Proceedings/TENCON, pp. 2102–2107, 2010.

[9] ZVEI - Zentralverband Elektrotechnik- und Elektronikindustrie e.V., "Gleichspannungsnetze in der industriellen Produktion," p. 12, 2017.

[10] K. Yotsumoto, S. Muroyama, S. Matsumura, and H. Watanabe, "Design for a Highly Efficient Distributed Power Supply System Based on Reliability Analysis," in 10th int. Telecommunications Energy Conf. 1988, pp. 545-550.

[11] "Steady State Availability," 2022. [Online]. Available: http://www.electropedia.org/iev/iev.nsf/display?openform&ievref=192-08-07

[12] A. Kwasinski, "Quantitative evaluation of DC microgrids availability: Effects of system architecture and converter topology design choices," IEEE Trans. Power Electron., vol. 26, no. 3, pp. 835–851, 2011.

[13] B. R. Shrestha, T. M. Hansen, and R. Tonkoski, "Reliability analysis of 380V DC distribution in data centers," 2016 IEEE Power Energy Soc. Innov. Smart Grid Technol. Conf. ISGT 2016, pp. 0–4, 2016.

[14] A. Lisnianski, I. Frenkel, and Y. Ding, Multi-State System Reliability Analysis and Optimization for Engineers and Industrial Managers. London: Springer, 2010.

[15] G. Abeynayake, T. Van Acker, D. Van Hertem, and J. Liang, "Analytical Model for Availability Assessment of Large-Scale Offshore Wind Farms including Their Collector System," IEEE Trans. Sustain. Energy, vol. 12, no. 4, pp. 1974–1983, 2021.

[16] E. Zio, The Monte Carlo Simulation Method for System Reliability and Risk Analysis. Springer, 2005.